Polymer 50 (2009) 789–795

Contents lists available at ScienceDirect

Polymer

journal homepage: www.elsevier.com/locate/polymer

Synthesis and characterization of highly refractive polyimides derived from 2,7-bis(4′-aminophenylenesulfanyl)thianthrene-5,5,10,10-tetraoxide and aromatic dianhydrides

Nam-Ho You, Yasuo Suzuki, Tomoya Higashihara, Shiji Ando, Mitsuru Ueda*

Department of Organic and Polymeric Materials, Graduate School of Science and Engineering, Tokyo Institute of Technology, 2-12-1, H-120, O-okayama, Meguro-ku, Tokyo 152-8552, Japan

ARTICLE INFO

Article history:
Received 23 September 2008
Received in revised form
22 November 2008
Accepted 1 December 2008
Available online 6 December 2008

Keywords:
Polyimide
High refractive index
Transparency

ABSTRACT

New polyimides (PIs) containing thioether and sulfonyl groups in their main chains have been developed. These PIs were synthesized by a two-step polycondensation procedure from several dianhydrides such as 4,4′-[*p*-thiobis(phenylenesulfanyl)] diphthalic anhydride (3SDEA), 4,4′-oxydiphthalic anhydride (ODPA), 4,4′-[sulfonylbis(phenylenesulfanyl)] diphthalic anhydride (pDPSDA) and a new sulfonyl and sulfur-containing aromatic diamine, 2,7-bis(4′-aminophenylenesulfanyl)thianthrene-5,5,10,10-tetraoxide (APTTT). All of the PIs show good thermal and optical properties such as optical transparency higher than 80% at 450 nm for a thickness of ca. 10 μm, glass transition temperatures higher than 250 °C, thermal decomposition temperatures ($T_{10\%}$) in the range of 504–514 °C. Because of the two sulfonyl groups at each monomer unit in the polymer main chain, all of the PIs show good transparency maintaining relatively high refractive index.

1. Introduction

High refractive index polymers have been developed in recent years for optoelectronic applications, such as coatings for long-period-grating (LPG) refractive index sensors [1], organic light-emitting diodes (OLEDs) [2], microlens components for charge coupled devices (CCD), and high performance CMOS image sensors (CISs) and so on [3,4]. According to the Lorentz–Lorenz equation [5], the refractive index values of conventional polymers, which are often in the range of 1.3–1.7, can be effectively tuned by the introduction of some substituents, such as aromatic rings [6], halogen atoms (except fluorine) [7], sulfur atoms, and metal atoms [8,9]. Recently, many sulfur-containing polymers based on conventional poly(methacrylates) [10], poly(ethylene glycol) [11], polyurethanes [12], and polyimides [13], have been developed for advanced integrated optical applications. In particular, polyimides (PIs) possess good combined properties, such as excellent thermal stability, high chemical resistance, and high mechanical properties.

Quite recently, sulfur-containing new polyimides have been prepared for optical application in our laboratory [14–18]. All of them exhibited excellent thermal stability, a high refractive index, good transparency, and low birefringence. However, when fabricating an optical device, deep coloration of polyimides, due to the charge-transfer (CT) interactions between the electron-donating diamine and the electron-accepting aromatic dianhydride groups is one of the serious obstacles [19]. Many efforts were made to decrease the coloration of conventional PIs such as the introduction of fluoro-containing substituents as strong electron-withdrawing groups[20,21]. However, most of these procedures often simultaneously lower the refractive indices of PIs. In our continuous effort to obtain further improved transparency while maintaining high thermal stability and high refractive indices, we designed and synthesized a new diamine, APTTT, with two sulfonyl groups included in the cyclic structure of the central part. The lower electron-donating property of APTTT, which is represented by a high ionization potential of 7.48 eV, may prevent CTC formation, which deteriorates transparency in the visible region. In addition, the bulky cyclic structure containing two sulfonyl groups weakens the intermolecular packing between PI chains, which should reduce the birefringence. Moreover, the sulfur atoms in the thioether units are endowed with high molar refractivity to maintain high refractive indices.

In this study, we report on the synthesis and characterization of optically transparent polyimides derived from APTTT and several dianhydrides, such as 3SDEA, ODPA, and pDPSDA. All of the PIs exhibit high refractive indices in the range of 1.7105–1.7374 with high thermal stability (>400 °C), low birefringence in the range of 0.0071–0.0095, and good transparency over 450 nm with transmittance higher than 80%. The structure–property relationships and refractive indices of the PIs are investigated in detail.

* Corresponding author. Tel./fax: +81 3 5734 2127.
E-mail address: ueda.m.ad@polymer.titech.ac.jp (M. Ueda).

0032-3861/$ – see front matter © 2008 Published by Elsevier Ltd.
doi:10.1016/j.polymer.2008.12.001

2. Experimental section

2.1. Materials

p-Fluorothiophenol and *p*-aminothiophenol were purchased from Wako, Japan. Fuming sulfuric acid (30% oleum) was purchased from Wako, Japan. *N*,*N*-Dimethylformamide (DMF) and *N*-methyl-2-pyrrolidone dehydrated (NMP) were used as-received. Periodic acid (H_5IO_6) and chromium trioxide (CrO_3) were purchased from Wako, Japan. All other chemicals were purchased from TCI and Wako, Japan. ODPA was dried in vacuum at 120 °C for 4 h prior to use. 3SDEA and pDPSDA were synthesized according to our previous works [18,22].

2.2. Measurements

The NMR spectra were recorded on a BRUKER DPX-300S spectrometer at the resonant frequencies at 300 MHz for ^1H and at 75 MHz for ^{13}C nuclei using $CDCl_3$ or DMSO-d_6 as solvent and tetramethylsilane as the reference. The ^{13}C DEPT (distortionless enhancement by polarization transfer) experiment was carried out using DMSO-d_6 as solvent. The FT-IR spectra were measured by a Horiba FT-120 Fourier transform spectrophotometer. The UV–visible optical transmission spectra were recorded on a Hitachi U-3210 spectrophotometer at room temperature. The transmittance of PI films peeled from substrates was evaluated in the wavelengths ranging 250–800 nm. Elemental analyses were performed on a Yanaco MT-6 CHN recorder elemental analysis instrument. Inherent viscosity was measured using an Ubbelohde viscometer with 0.5 g/dL NMP solution at 30 °C. The thermal properties were estimated from a Seiko TG/DTA 6300 thermal analysis system (TGA), and a Seiko DSC 6300 differential scanning calorimetry (DSC) under nitrogen atmosphere at a heating rate of 10 °C/min. Melting points of all monomers were recovered using DSC analysis unless otherwise indicated. Dynamic mechanical thermal analyses (DMA) were developed on PI films (30 mm long, 10 mm wide and 50–80 μm thick) on a Seiko DMS 6300 instrument at a heating rate of 2 °C/min with a load frequency of 1 Hz in air. The glass transition temperature values (T_gs) were determined as the peak temperature of the loss modulus (E'') plot. The in-plane (n_{TE}) and out-of-plane (n_{TM}) refractive indices of PI films were measured with a prism coupler (Metricon, model PC-2000) equipped with a He–Ne (wavelength: 633 nm) and semiconductor lasers (845, 1324, and 1558 nm) and the corresponding half-waveplates in the light-path. The in-plane/out-of-plane birefringence (Δn) was calculated as a difference between n_{TE} and n_{TM}. The average refractive index was calculated according to equation: $n_{AV} = [(2n_{TE}^2 + n_{TM}^2)/3]^{1/2}$. All the films were dried at 100 °C for 30 min under vacuum before testing to remove the absorbed moisture.

2.3. DFT calculation

Refractive indices of the pure PIs are to be calculated using the Lorentz–Lorenz equation, which is given as follows:

$$\frac{n^2-1}{n^2+2} = \frac{4\pi}{3}\frac{\rho \cdot N_A}{M_w}\alpha = \frac{4\pi}{3}\frac{\alpha}{V_{mol}} = \frac{4\pi}{3}K_p\frac{\alpha}{V_{vdw}} \quad (1)$$

where n is the refractive index; ρ, the density; N_A, the Avogadro number; M_w, the molecular weight; α, the linear molecular polarizability; V_{mol}, the molecular volume; V_{vdw}, the van der Waals volume; and K_p, the packing coefficient. The 6-311G(d) basis set was used for the geometry optimizations under no constraints, and the 6-311++G (d, p) was used for calculations of linear polarizabilities. The three-parameter Becke-style hybrid functional (B3LYP) was adopted as a functional, and all the calculations were performed using the Gaussian-03 software package (Rev.C02 and D01). A typical packing coefficient (K_p) of 0.60 was used for evaluating the intrinsic molecular volumes of models to predict the refractive indices [23]. The molecular orbital energies, ionization potentials, and molecular polarizabilities of sulfur-containing diamines were also calculated in the same manner as the models for PIs. The ionization potentials (Ip) were estimated as the differences in total energy between the neutral state and the cation state with the same molecular geometry. The total energies in the cation states were calculated within the framework of the unrestricted DFT method.

Table 1
Electronic properties and molecular polarizability of sulfur-containing diamines calculated by DFT theory (B3LYP/6-311++G (d, p)).

Diamine	ε_{HOMO}[a] (eV)	Ip[b] (eV)	α[c] (Å^3)	V_{vdw}[d] (Å^3)	α/V_{vdw}	n_{av}[e] (3SDEA–PIs)
BADPS	−5.99	7.10	58.49	391.7	0.1493	1.7326
APTTT	−6.40	7.48	63.82	414.5	0.1540	1.7374
3SDA	−5.38	6.63	58.15	377.0	0.1542	1.7482
APTT	−5.52	6.73	62.62	384.1	0.1630	1.7600
APDBT	−5.33	6.62	59.80	365.0	0.1638	1.7578

[a] Molecular orbital energy of HOMO.
[b] Ionization potential.
[c] Molecular polarizability.
[d] van der Waals volume.
[e] Average refractive index (measured at 633 nm) of the PIs prepared from 3SDEA dianhydride and the corresponding diamine.

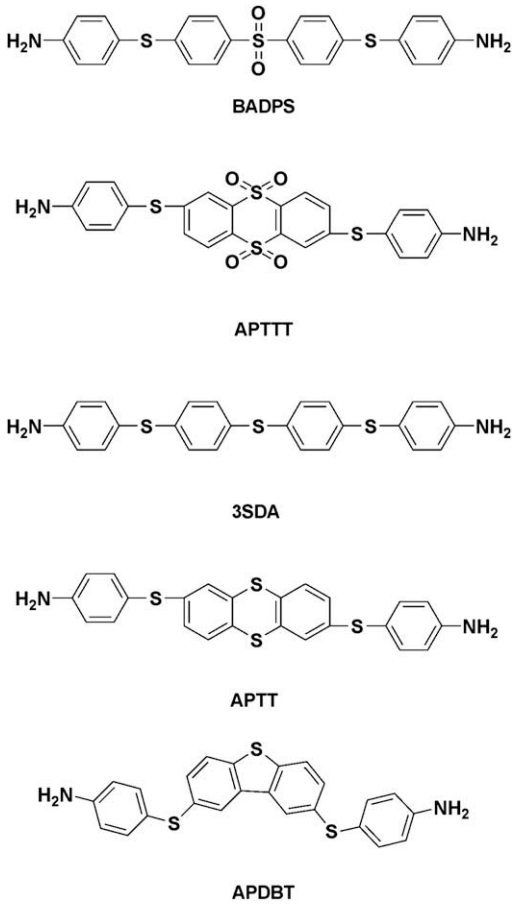

Scheme 1. Structures of sulfur-containing diamines which afford high refraction to polyimides.

2.4. Synthesis of monomer (Scheme 2)

2.4.1. 2,7-Difluorothianthrene (2,7-DFT)

The compound was synthesized according to the reported procedure [23]; mp: 156 °C (DSC peak temperature) (lit. [23] 156 °C); ^{1}H NMR (300 MHz, $CDCl_3$, ppm): 6.96–7.03 (m, 2H), 7.22–7.25 (m, 2H), 7.41–7.45 (m, 2H).

2.4.2. 2,7-Difluorothianthrene-5,10-tetraoxide (2,7-DFTT)

H_5IO_6 (7.22 g, 31.68 mmol) was dissolved in acetonitrile (120 mL) at room temperature for 30 min, and then, CrO_3 (0.16 mmol, 15 mg) was added to a solution. The mixture was stirred for 30 min. To this solution was added a solution of 2,7-difluorothianthrene (1.00 g, 3.96 mmol) in acetonitrile (20 mL) at room temperature for 5 h. After the reaction, the crude product was filtered and washed with methanol. The crude product was purified by recrystallization from DMF and water (5/1, v/v) to give white crystals. Yield: 1.06 g (85%): mp 270 °C (DSC peak temperature); ^{1}H-NMR (300 MHz, DMSO-d_6, ppm): $\delta = 8.30$ (m, 2H), 8.15 (m, 2H), 7.78 (m, 2H). Anal. Calcd. for $C_{12}H_6F_2O_4S_2$; (316.30): C, 45.57; H, 1.91. Found: C, 45.15; H, 2.05.

2.4.3. 2,7-Bis(4′-aminophenylenesulfanyl)thianthrene-5,10-tetraoxide (APTTT)

To a solution of *p*-aminothiophenol (0.92 g, 7.37 mmol) in DMF (10 mL) was added potassium carbonate (1.22 g, 8.85 mmol). To this solution was added 2,7-DFTT (1.06 g, 3.35 mmol) in room temperature for 5 h. After the reaction, the obtained solid was poured into water. The precipitated solid was filtered and washed with methanol. The crude solid was purified by recrystallization from methoxyethanol and water (10/1, v/v) to yield pale yellow crystals. Yield: 1.40 g (79.5%); mp: 261 °C (DSC peak temperature). ^{1}H-NMR (300 MHz, DMSO-d_6, ppm): $\delta = 8.05$ (d, 2H), 7.60 (d, 2H), 7.50 (m, 2H), 7.24 (d, 4H), 6.70 (d, 4H), 5.79 (s, 6H). ^{13}C-NMR (DMSO-d_6, ppm): $\delta = 151.8$, 151.6, 139.5, 137.3, 133.4, 129.5, 126.9, 120.5, 115.7, 110.4. Anal. Calcd. for $C_{24}H_{18}N_2O_4S_4$; (526.67): C, 54.73; H, 3.44. Found: C, 54.77; H, 3.64.

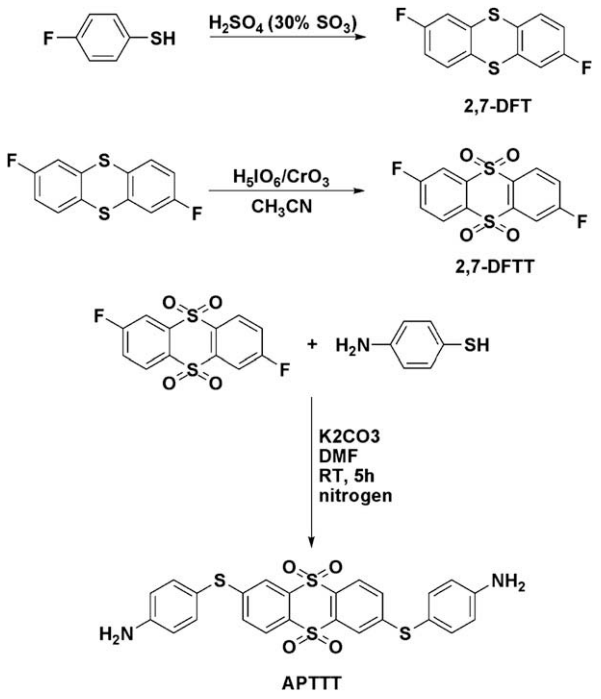

Scheme 2. Synthetic route for the preparation of APTTT.

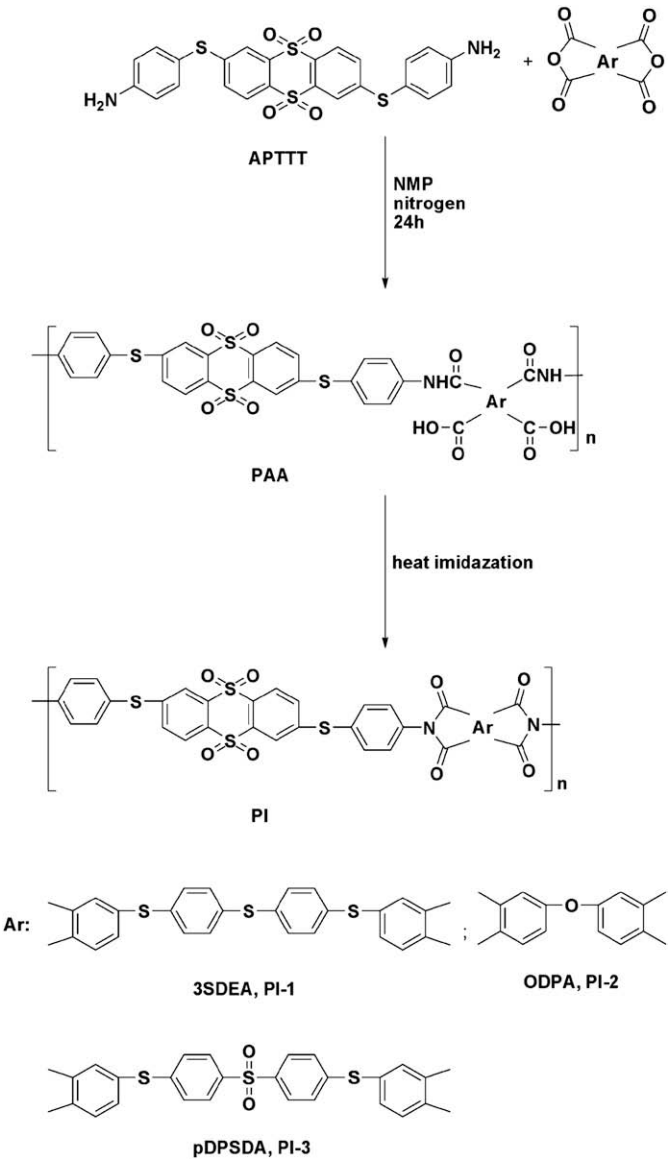

Scheme 3. Synthesis of polyimides.

2.5. Polyimide synthesis (Scheme 3)

A typical polymerization procedure for the synthesis of poly(amic acid) (PAA) can be illustrated by PI-1 as follows. APTTT (0.5266 g, 1.00 mmol) previously dried at 100 °C for 4 h and dehydrated NMP (1.3 g) were charged into a 20 mL flask equipped with a magnetic stirrer in a nitrogen atmosphere (Scheme 3). 4′,4′-[*p*-Thiobis(phenylsulfanyl)]diphthalic anhydride (3SDEA) (0.5426 g, 1.00 mmol) was added and dehydrated NMP (3.0 g) was used to adjust the solid content of the reaction systems to 20 wt%. The solution was stirred at room temperature for 48 h to give a viscous PAA solution, which was filtered through a 0.45 μm Teflon syringe filter.

To control the film thickness, the PAAs solutions were spin-coated on fused silica substrates and silicon wafers at different spinning rate, respectively. The thickness of PI films was controlled to be ~10 μm for UV–vis and FT-IR measurements. To measure thermal properties, the thickness of PI films was adjusted from 50 to 100 μm. All of the PI films were prepared by thermal imidization of PAA solutions (Scheme 3). PI-1 film was obtained by thermal

curing of the PAA-1 solution in an oven for 1–2 h each step at 80, 120, 150, 200, 250 °C and 30 min at 300 °C, respectively, followed by immersing the silicon wafers into warm water. The films of PI-2 and PI-3 were prepared by a similar process from PAA solutions, respectively.

3. Results and discussion

3.1. Electronic properties of diamines

The authors have clarified that the HOMO levels (ε_{HOMO}) and/or ionization potentials (Ip) of source materials (diamines) are closely related to the optical transparency of PIs [20,21]. The HOMO of PIs is generally located on the diamine moieties including imide nitrogen, and the LUMO is located on the dianhydride moiety. The CT interactions between the HOMO and LUMO of aromatic PIs cause weak but broad and significant absorption in the longer wavelength region. Thereby, the optical transmittance of PIs in the visible region can be predicted or inferred from the electronic properties of the source materials. Table 1 lists the calculated electronic properties of the sulfur-containing diamines, the structures of which are depicted in Scheme 1. These diamines developed by the authors can yield highly refractive PIs due to the high refractivity of sulfur atoms [13–18]. In particular, the APTTT diamine designed in this study shows the lowest HOMO energy and the highest Ip value, which indicates that APTTT possesses the lowest electron-donating property among the five diamines in Table 1. This should significantly weaken the intra- and intermolecular CT interactions. It has been reported that the CTC formation in the ground state causes a tailing of the optical absorption of PIs to longer wavelengths [19–21], and it deteriorates the transparency in the visible region. In addition, the cyclic structure containing two sulfonyl groups at the center of APTTT should reduce the intermolecular packing between PI chains, which in turn should decrease the birefringence. According to Eq. (1), the refractive index of PI monotonically increases with an increase in the parameter of α/V_{vdw}. As listed in Table 1, the α/V_{vdw} value of APTTT is slightly larger than that of BADPS, having one sulfonyl group, but smaller than those of 3SDA, APTT, and APDBT containing thioether linkages. The relatively small α/V_{vdw} value of APTTT apparently originates from the significant increase in V_{vdw} due to the bulky sulfonyl groups. In particular, the α value of APTTT is close to that of APTT (difference is 1.9%), but the V_{vdw} of APTTT is larger than that of APTT by 7.9%. APTTT shows the largest V_{vdw} among the five diamines.

3.2. Synthesis of monomers

APTTT was synthesized by a three-step procedure, as shown in Scheme 2. Firstly, 2,7-DFT was prepared in a similar way to the previously reported procedure [24]. Secondly, the oxidation of 2,7-DFT was carried out with H_5IO_6/CrO_3 to yield 2,7-difluorothianthrene-5,5,10,10-tetraoxide (2,7-DFTT) [25]. Finally, 2,7-DFTT was reacted with aminothiophenol to yield APTTT at room temperature. The structure of APTTT was characterized by IR absorption and NMR spectroscopies. The IR spectrum of 2,7-DFTT shows the characteristic absorption peaks due to the sulfone group at 1352 and 1165 cm^{-1}. On the other hands, the spectrum of APTTT exhibits the characteristic absorptions at 3478 and 3372 cm^{-1} due to the N–H stretching of a primary amino group as shown in Fig. 1.

The ^1H- and ^{13}C-NMR spectra of APTTT are presented in Fig. 2 with assignments of all peaks. The signal at 5.79 ppm in Fig. 2a is assignable to the amino groups. The hydrogens attached to the aromatic ring having sulfonyl groups (Ha, Hb, Hc) are observed at 8.04, 7.60 and 7.50 ppm in the spectrum. The hydrogens of the aromatic rings containing an amino moiety are observed at 7.23 and 6.69 ppm. In the ^{13}C NMR spectrum (Fig. 2b), ten carbon signals, which are consistent with the expected structure, are observed. Among these peaks, five signals are readily assigned to quaternary carbons by DEPT-135 measurement. In addition, elemental analysis clearly supported the formation of the diamine.

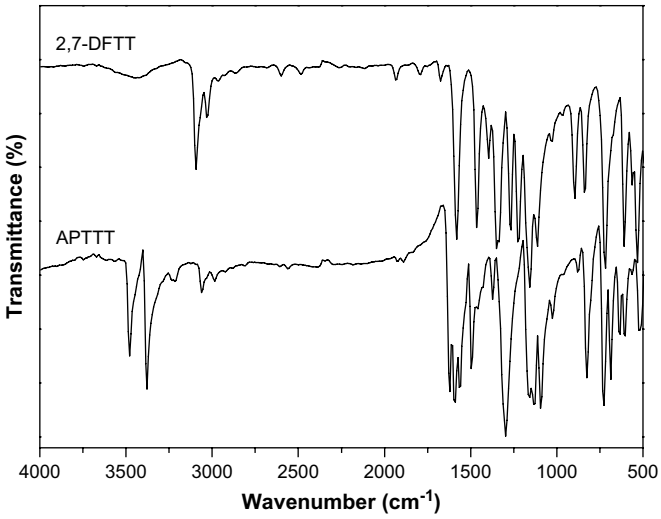

Fig. 1. FT-IR spectra of 2,7-DFTT and APTTT.

3.3. Synthesis and characterization of polyimides (PIs)

A series of PIs were synthesized by employing a two-step polycondensation of aromatic dianhydrides, such as 3SDEA, ODPA, and pDPSDA with APTTT via soluble poly(amic acid) (PAA) precursors, followed by thermal imidization at elevated temperatures (Scheme 3). PAAs, which have inherent viscosities in the

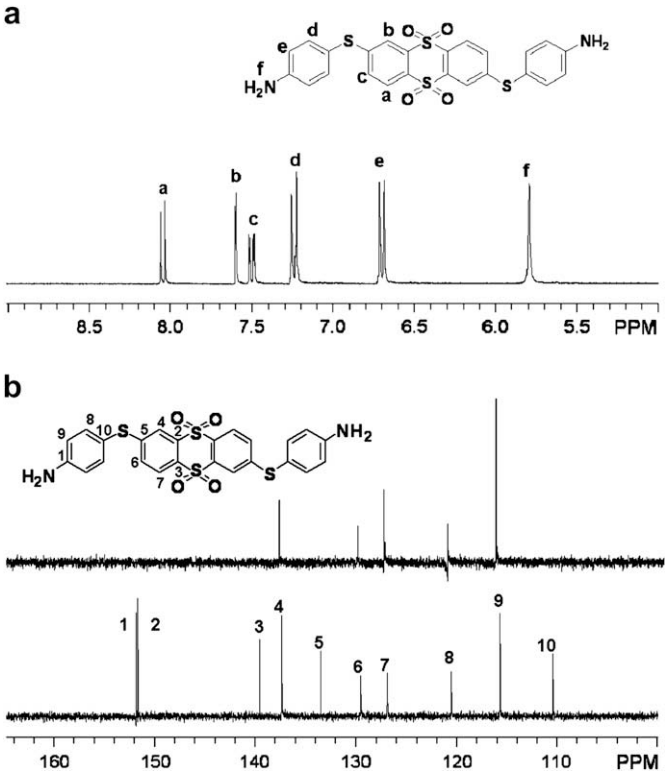

Fig. 2. NMR spectra of APTTT (a) ^1H NMR; (b) ^{13}C NMR and DEPT-135.

Table 2
Synthesis and characterization of polyimides.

PI	$[\eta]_{inh}$PAA[a] (dL/g)		Elemental analysis		
			C (%)	H (%)	N (%)
PI-1	0.51	Calcd.	60.33	2.92	2.71
		Found	59.32	2.99	2.80
PI-2	0.49	Calcd.	59.84	2.76	3.49
		Found	59.07	2.91	3.63
PI-3	0.26	Calcd.	58.52	2.83	2.62
		Found	57.81	2.96	2.73

[a] Measured at a concentration of 0.5 g/dL of NMP solution at 30 °C.

Table 3
Thermal properties of the polyimides.

PI	S[a] (wt%)	Film[b]	T_g[c] (°C)		$T_{5\%}$[d] (°C)	$T_{10\%}$[d] (°C)
			DSC	DMA		
PI-1	21.68	Pale-yellow	250	245	488	514
PI-2	15.98	Pale-yellow	299	292	469	508
PI-3	21.03	Pale-yellow	271	262	475	504

[a] Sulfur content.
[b] Color at the thickness of approximately 10 μm.
[c] T_g: glass transition temperature.
[d] $T_{5\%}$ $T_{10\%}$: temperatures at 5% and 10% weight loss, respectively.

range of 0.51–0.26 dL/g, are produced (Table 2). Although the inherent viscosity of PI-3 was relatively low, it also gave a self-standing film probably due to many flexible thioether linkages.

PI films were prepared by thermal imidization of the PAAs cast onto silicon wafers and quartz plates under nitrogen, followed by immersion in warm water. Successful thermal conversion from PAAs to PIs was confirmed by the FT-IR spectra and are shown in Fig. 3. The characteristic absorptions which originated from the imide moiety are observed at 1770 cm^{-1} ($\upsilon_{as,C=O}$), 1720 cm^{-1} ($\upsilon_{s,C=O}$), and 1370 cm^{-1} (υ_{C-N}). The typical absorption peaks of the sulfonyl groups are revealed at 1168 and 1320 cm^{-1}. Furthermore, the exact structures of the PIs were confirmed by elemental analysis (Table 2).

3.4. Thermal properties

The thermal decomposition and deformation behavior of all PIs were evaluated by TGA, DSC, and DMA measurements under nitrogen. The results are presented in Table 3. As shown in Fig. 4 (TGA), all PIs showed good thermal stability, such as 5%-weight-loss temperatures ($T_{5\%}$) in the range of 469–488 °C and $T_{10\%}$ in the range of 504–514 °C. The glass transition temperatures (T_gs) estimated by DSC (Fig. 5) and DMA (Fig. 6) are close to each other. All PIs show high T_gs of more than 250 °C as measured by DSC. In particular, PI-2 has the highest T_g, which is 49 °C higher than that of PI-1 owing to the rigid structure of the polymer main chain. Additionally, DMA analyses were performed under air at a heating rate of 2 °C/min. Fig. 6 shows the variations in the storage modulus (E'), loss modulus (E'') and loss factor ($\tan\delta$) at different temperatures. It can be seen from Fig. 6a that the modulus remains constant or decreased slightly on heating over a wide temperature range up to 200 °C. The corresponding E'' curves, which are determined as the peak temperatures, exhibit a similar trend.

3.5. Optical properties

Fig. 7 shows the UV–vis absorption spectra of PI films (pale-yellow, ~10 μm thick). As listed in Table 4, the cutoff wavelengths (λ_{cutoff}) of the films are in the range of 399–373 nm. The transmittances of the PI films measured at 450 nm are higher than 80% in the visible region, which is much better than that of the reference PI (ref-PI) derived from 3SDEA and 2,7-bis(4′-aminophenylenesulfanyl)thianthrene (APTT) [26]. The high transparency of all PIs originates from the reduction of intermolecular interactions by bulky sulfonyl groups in the main chain and the reduction of the intra- and intermolecular CT interactions. As can be seen in Fig. 7 and Table 4, the optical transmittance at 450 nm for PI-2, which shows the shortest λ_{cutoff}, is the highest in the three PIs. In addition, it is noteworthy that PI-3 having a sulfonyl linkage in the dianhydride moiety exhibits a higher transmittance (87%) than that of PI-1 despite the almost same λ_{cutoff} values. The high transmittance of PI-3 at 450 nm can be ascribed to the reduction of CT interactions in this PI because the CT absorptions are generally observed in the longer wavelength region than λ_{cutoff}.

As listed in Table 4, the in-plane (n_{TE}) and out-of-plane (n_{TM}) refractive indices of the PI films measured at 633 nm range from 1.7137 to 1.7402 and 1.7041 to –1.7318, respectively. The fact that the n_{TE} values are slightly higher than the n_{TM} ones for all PI films reflects the preferential chain orientation parallel to the film plane. The average refractive indices (n_{av}) estimated from the n_{TE} and n_{TM} values range between 1.7106 and 1.7374 in the order of PI-1 > PI-3 > PI-2. This trend agrees with that of the sulfur content, though it

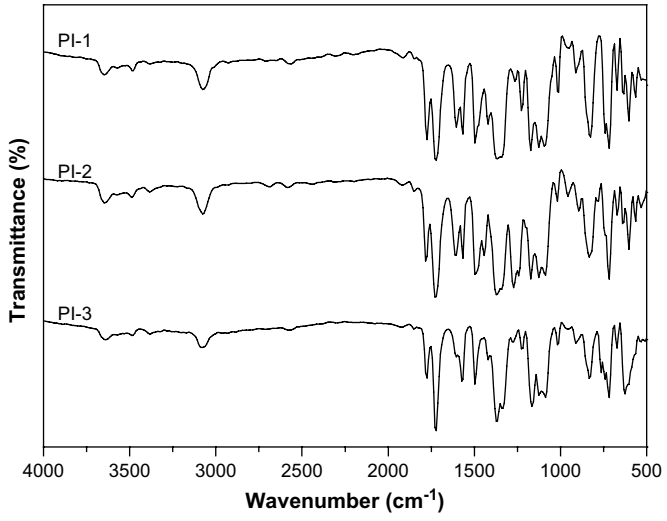

Fig. 3. FT-IR spectra of PI films.

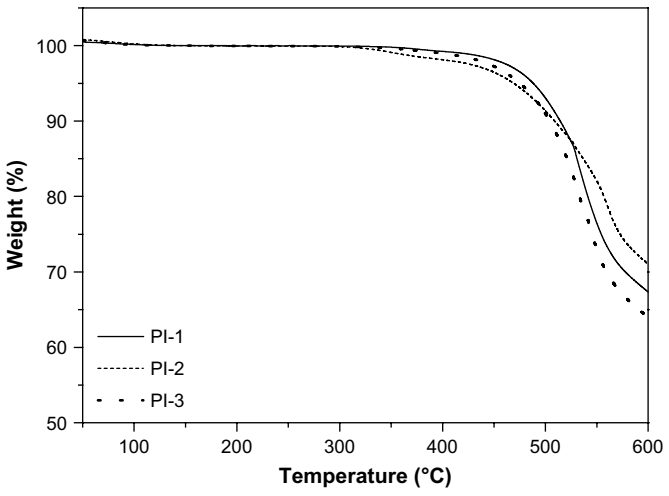

Fig. 4. TGA curves of PI films (in nitrogen atmosphere, 10 °C/min).

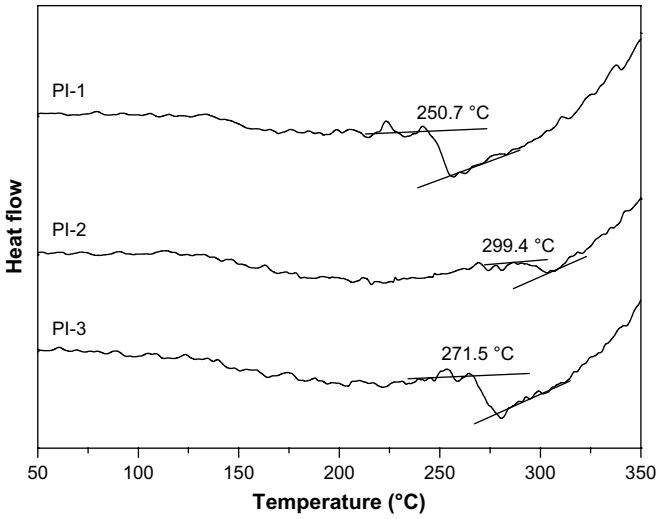

Fig. 5. DSC curves of PI films (in nitrogen atmosphere, 10 °C/min).

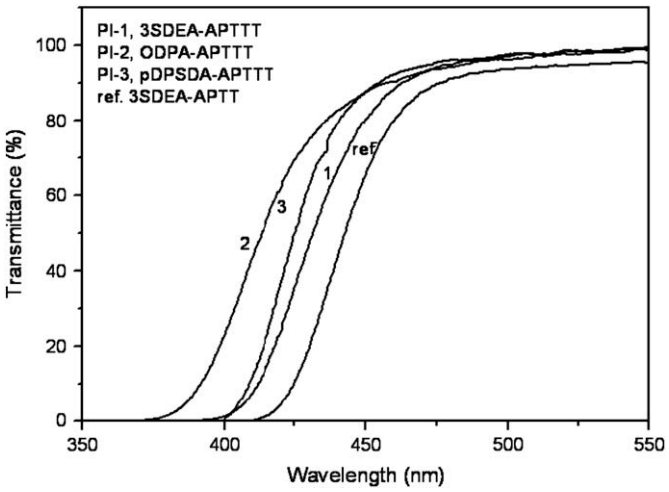

Fig. 7. UV–vis spectra of PI films (film thickness: ~10 μm).

has been discussed that the refractive indices of PIs are affected by several factors, including molecular geometry, molecular polarizability per volume (α/V_{vdw}), chain linearity or flexibility of polymer backbone, and degree of molecular packing (K_p) [10]. The ref-PI with the highest sulfur content shows the highest n_{av} at 1.7600. The calculated α/V_{vdw} values for PI-1, PI-2, PI-3, and ref-PI are 0.1645, 0.1564, 0.1581, and 0.1679, respectively, and those are proportional to the calculated refractive indices (n_{cal}), as listed in Table 4. The orders of α/V_{vdw} and n_{cal} coincide well with that of the experimental n_{av}, which demonstrates that the average refractive indices of these PIs are primarily determined by the molecular polarizability per volume. However, the deviation between n_{av} and n_{cal} is relatively larger for PI-1 than those for PI-2 and PI-3. This is also reflected in the fact that the K_p value estimated from the n_{av} and the calculated α/V_{vdw} for PI-1 (0.584) is significantly smaller than those of PI-2 (0.597) and PI-3 (0.597). The relatively lower molecular packing of PI-1 can be also ascribed to the repeating sulfonyl linkages in the anhydride moiety of PI.

On the other hand, as shown in Table 1, the average refractive indices (n_{av}), measured at 633 nm for the PIs derived from 3SDEA dianhydride and the diamines in Scheme 1, show a monotonic increase in the values of α/V_{vdw} of the diamines. The n_{av} of PI-1 (3SDEA–APTTT) is slightly lower than those of the 3SDEA–PIs derived from 3SDA, APTT, and APDBT diamines, but higher than that of 3SDEA–BADPS. Furthermore, the calculated values of α/V_{vdw} for 3SDEA-PIs from BADPS, APTTT (PI-1), 3SDA, APTT (ref-PI), and APDBT PIs are 0.1606, 0.1645, 0.1655, 0.1679, and 0.1655, respectively. This order also agrees with that of the experimental n_{av} values. The slightly higher n_{av} values observed for the latter three 3SDEA-PIs are sacrificed by their lower optical transparency in the visible region [14,16,18].

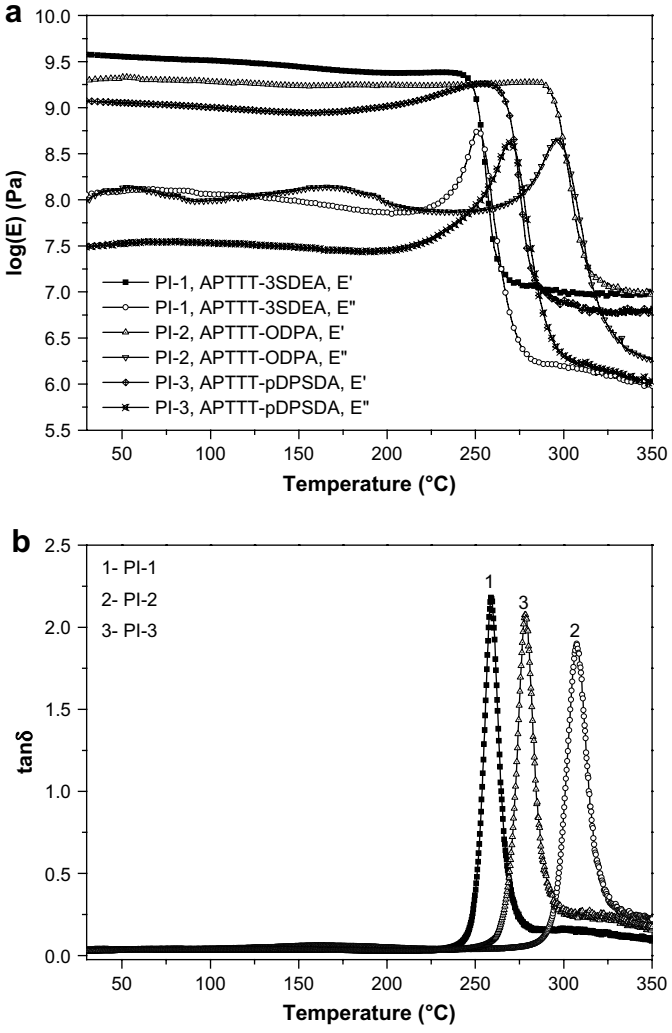

Fig. 6. DMA curves of PI-1, PI-2, and PI-3 (1 Hz, 2 °C/min): (a) modulus (b) tan δ.

Table 4
Optical properties of the PIs films.

PI	λ_{cutoff}[a] (nm)	d[b] (μm)	Refractive indices and birefringence at 633 nm[c]				n_∞[d]	D[e] ($\times 10^4$)	n_{cal}[f]
			n_{TE}	n_{TM}	n_{av}	δn			
PI-1	399	12.4	1.7402	1.7318	1.7374	0.0084	1.6834	21.17	1.765
PI-2	373	12.9	1.7137	1.7041	1.7106	0.0096	1.6587	19.59	1.715
PI-3	398	7.8	1.7232	1.7162	1.7209	0.0071	1.6705	20.45	1.726
ref-PI[g]	466	11.9	1.7628	1.7545	1.7600	0.0084	1.7034	22.57	1.786

[a] Cut-off wavelength.
[b] Film thickness for refractive index measurement.
[c] Measured at 632.8 nm, see *Measurements*.
[d] Refractive index at the infinite wavelength.
[e] Dispersion coefficient of refractive index obtained from the fitting by the simplified Cauchy formula ($n_\lambda = n_\infty + D\lambda^2$).
[f] Calculated refractive index (see Section 2.3).
[g] 3SDEA-APTT PI (Ref. [24]).

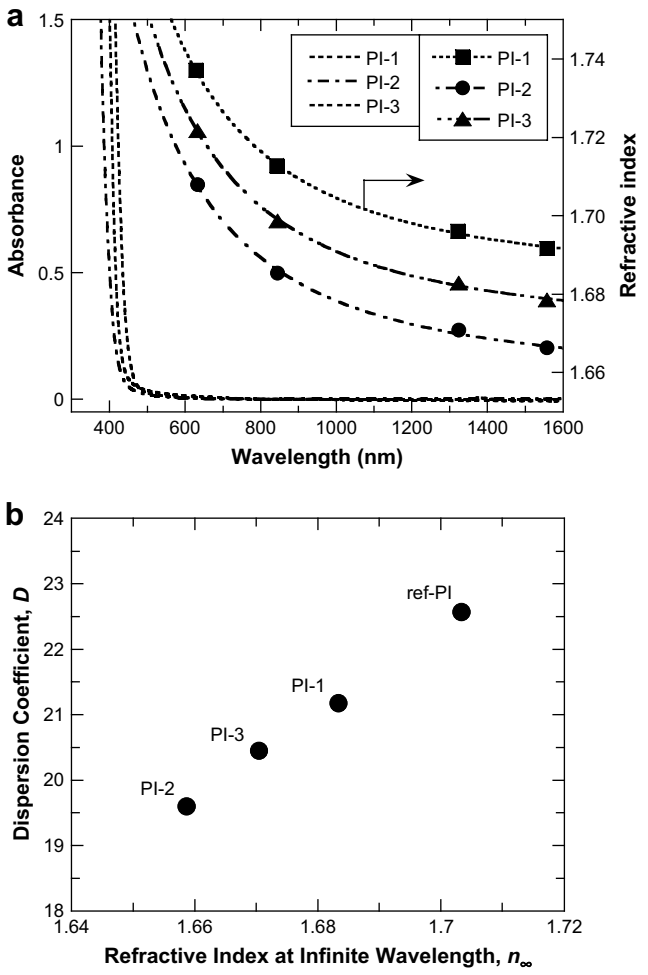

Fig. 8. (a) Optical absorption and (b) wavelength dispersion of refractive indices of PIs.

Fig. 8a shows the plots of the wavelength-dependent n_{av} values measured at 633, 845, 1324, and 1558 nm for PI-1 to PI-3. The dispersions of n_{av} were fitted by a simplified Cauchy formula.

$$n_\lambda = n_\infty + \frac{D}{\lambda^2}, \tag{2}$$

where λ is the wavelength, n_∞ is the estimated refractive index at infinite wavelength, and D is the coefficient of dispersion. The values of n_∞ and D are listed in Table 4. A larger D indicates a larger wavelength dispersion, and a high n_∞ corresponds to an inherently high refractive index without the influence of absorptions located at shorter wavelengths. As shown in Fig. 8b, the values of D are linearly proportional to those of n_∞, and the order in n_∞ is the same as that in n_{av} measured at 633 nm. The linear relationship between D and n_∞ had been reported by the authors [27] which clearly shows the trade-off relation between the refractive index at the infinite wavelength and the wavelength dispersion. In other words, we can choose an appropriate combination of n_∞ and D by varying the dianhydride moiety of the aromatic PIs.

Furthermore, both of the bulky sulfone and thioether linkages in the molecular chains of the PIs (PI-1 to PI-3), including the ref-PI, endow them with low Δn in the range of 0.0071–0.0084. Note that the PIs derived from APTTT, having a planar and two-dimensionally polarizable cyclic structure with two sulfonyl linkages, exhibit significantly small values of Δn. This indicates that the introduction of the sulfonyl linkage is an effective way to prevent the in-plane orientation of PI chains. Such optically isotropic PI films are desirable for advanced optical fabrications in micro-optics, waveguides, and optical circuit applications.

4. Conclusions

A new diamine, APTTT, was synthesized and polymerized with sulfur-containing aromatic dianhydrides such as 3SDEA, ODPA, and pDPSDA to afford high transparency. All PIs show high thermal properties and refractive index values in the range from 1.7106 to 1.7374. Although the PIs based on APTTT exhibit lower refractive indices than those of 3SDEA–APTT due to the sulfonyl groups in the main chain, all PIs show improved optical transparency exceeding 80% at 450 nm. These PIs can be good candidates as advanced optical application components.

References

[1] Cusano A, Pilla P, Contessa L, Campopiano S, Cutolo A, Giordano M. Proc SPIE 2005;5952. 59521C/1–59521C/10.
[2] Ju YG, Almuneau G, Kim TH, Lee BW. Jpn J Appl Phys 2006;45:2546–9.
[3] Suwa M, Niwa H, Tomikawa M. J Photopolym Sci Technol 2006;19:275–6.
[4] Regolini JL, Benoit D, Morin P. Microelectron Relia 2007;47:739–42.
[5] Ando S, Fujigaya T, Ueda M. Jpn J Appl Phys 2002;41:L105–8.
[6] Shinichi K. Masashi T. Hiroaki M. Takeshi F. Kana K. Misuaki Y. et al. Kokai Tokkyo JP 2005162785; 2005.
[7] Minns RA, Gaudiana RA. J Macromol Sci Pure Appl Chem 1992;A29:19–30.
[8] Okutsu R, Ando S, Ueda M. Chem Mater 2008;20:4017–23.
[9] Liu J, Nakamura Y, Ogura T, Shibasaki, Ando S, Ueda M. Chem Mater 2008; 20:273–81.
[10] Matsuda T, Funae Y, Yoshida M, Yamamoto T, Takaya T. J Appl Polym Sci 2000; 76:45–9.
[11] Lu CL, Cui ZC, Wang YX, Yang B, Shen JC. J Appl Polym Sci 2003;89:2426–30.
[12] Nebioglu A, Leon J, Khudyakov IV A. Ind Eng Chem Res 2008;47:2155–9.
[13] Liu JG, Shibasaki Y, Ando S, Ueda M. High Perform Polym 2008;20:221–37.
[14] Liu JG, Nakamura Y, Terraza CA, Suzuki Y, Shibasaki Y, Ando S, et al. Macromol Chem Phys 2008;209:195–203.
[15] Liu JG, Nakamura Y, Shibasaki Y, Ando S, Ueda M. Polym J 2007;39:543–50.
[16] Liu JG, Nakamura Y, Suzuki Y, Shibasaki Y, Ando S, Ueda M. Macromolecules 2007;40:7902–9.
[17] Terraza CA, Liu JG, Nakamura Y, Shibasaki Y, Ando S, Ueda M. J Polym Sci Part A Polym Chem 2008;46:1510–5120.
[18] Liu JG, Nakamura Y, Shibasaki Y, Ando S, Ueda M. J Polym Sci Part A Polym Chem 2007;45:5606–17.
[19] Groh W, Zimmerman A. Macromolecules 1991;24:6660–3.
[20] Ando S, Masuura T, Sasaki S. J Polym Sci Part A Polym Chem 1991;30:2285–93.
[21] Ando S, Masuura T, Sasaki S. Polym J 1997;29:69–76.
[22] Suzuki Y, Liu J, Nakamura Y, Shibasaki Y, Ando S, Ueda M. Polym J 2008; 40:414–20.
[23] Terui Y, Ando S. J Photopolym Sci Technol 2005;18:337–40.
[24] Edson JB, Knauss DM. J Polym Sci Part A Polym Chem 2004;42:6353–63.
[25] Liang X, Jie C, Mark LT. J Org Chem 2003;68:5388–91.
[26] Liu JG, Nakamura Y, Shibasaki Y, Ando S, Ueda M. Macromolecules 2007; 40:4614–20.
[27] Ando S, Watanabe Y, Matsuura T. Jpn J Appl Phys Part 1 2002;41:5254–8.